A Parameter Study for Static and Dynamic Denting

Dong-Won Jung*
Department of Mechanical Engineering, Cheju National University, 1, Ara 1(il)-dong, Jeju-do 690-756, Korea
M. J. Worswick
Department of Mechanical Engineering, University of Waterloo, Waterloo, Ontario, N2L 3G1, Canada

A parametric study of the factors controlling static and dynamic denting, as well as local stiffness, has been made on simplified panels of different sizes, curvatures, thicknesses and strengths. Analyses have been performed using the finite element method to predict dent resistance and panel stiffness. A parametric approach is used with finite element models of simplified panels. Two sizes of panels with square plan dimensions and a wide range of curvatures are analysed for several combinations of material thickness and strength, all representative of automotive closure panels. Analysis was performed using the implicit finite element code, LS-NIKE, and the explicit dynamic code, LS-DYNA for the static and dynamic cases, respectively. Panel dent resistance and stiffness behaviour are shown to be complex phenomena and strongly interrelated. Factors favouring improved dent resistance include increased yield strength and panel thickness. Panel stiffness also increases with thickness and with higher curvatures but decreases with size and very low curvatures. Conditions for best dynamic and static dent performance are shown to be inherently in conflict; that is, panels with low stiffness tend to perform well under impact loading but demonstrate inferior static dent performance. Stiffer panels are prone to larger dynamic dents due to higher contact forces but exhibit good static performance through increased resistance to oil canning.

Key Words: Static Denting, Dynamic Denting, Parameter Study, Finite Element Method, Panel Stiffness

1. Introduction

High stiffness and good dent resistance are desirable performance features of automotive body panels. These have been largely achieved in the past by evolutionary design, but with the push for lighter weight designs and the introduction of new body panel materials, such as aluminum alloy sheet, there exists a need for better understanding of the mechanical and material parameters governing panel stiffness and dent resistance. Panel dent resistance and stiffness have been the topics of numerous investigations but because of the complexity of the problem, a full understanding is still being pursued. To help advance this requirement, the present study has been undertaken on a parametric basis considering simplified panels analysed using finite element techniques.

There has been considerable experimental work on panel stiffness and dent resistance of steels (Johnson and Schaffnit, 1973; DiCello and George, 1974; Burley et al., 1976; Rolf et al., 1976) and aluminums (Burley and Niemeier, 1977; Neimeier and Burley, 1978; Mahmood,

* Corresponding Author,
E-mail: jdwcheju@cheju.ac.kr
TEL: +82-64-754-3625; **FAX**: +82-64-756-3886
Department of Mechanical Engineering, Cheju National University, 1, Ara 1(il)-dong, Jeju-do 690-756, Korea.
(Manuscript **Received** June 18, 2004; **Revised** September 15, 2004)

1981); however, there is a lack of data for autobody panels. Vadhavkar et al.(1981) and Swenson and Traficante (1982) started using analytical equations to predict dent phenomena. In the following years, much of the efforts for better prediction of panel stiffness and dent resistance have been concentrated on finite element analysis and experimental approach. Recent studies have highlighted both the static and dynamic denting characteristics of steels, as in Shi et al. (1997). Experimental examination of both static and dynamic denting of aluminum sheet has been presented by Thorburn (1994). Finite element modelling of dent responses can be found for various static test cases. Limited work on modelling of dynamic denting can be found in the literature (Vreede et al., 1995; Thomas et al., 1999; Jung, 2002). Ekstrand and Asnafi (1998) have looked to quantify the effects of structural support boundary conditions on dent resistance to some extent.

Although stiffness is a significant performance feature in its own right, relating to such things as "feel" and flutter and usually specified in terms of a limiting deformation under a given load, it is considered here in combination with denting primarily because it is known that stiffness has a major influence on denting performance. For this purpose, it is more meaningful to define stiffness as the slope of the load-deformation curve at a given load or alternatively as the slope of the straight line from the origin to a given point on the load-deformation curve, referred to as the secant stiffness.

Denting is defined as the residual local deformation of a panel due to a static or dynamic load. Static denting involves a slowly applied force at a point or on a small area such as may occur when an object is placed on a hood or pressed into a fender. Dynamic denting occurs under impact loading, such as during a hail storm or collision with a shopping cart. The essential difference is that static denting involves a "slowly" imposed force or deformation while dynamic denting involves a given impact energy. There are no commonly defined or accepted denting performance requirements among automobile manufacturers, nor are individual requirements generally known or published.

For the study of stiffness and denting, a parametric array of panels has been analysed. The panels are highly simplified relative to real automobile components but allow variations of those parameters that are thought to influence stiffness and denting. Panels of two sizes are considered, all square in plan and with fixed edges, combined with double curvatures ranging from highly curved (R=100 mm) to flat. Three thicknesses of aluminum alloy sheet material typical of automotive panels are considered, with the assumption that there has been no thinning during forming. All of the panels are assumed to be AA6111 alloy, but with properties ranging from the T4 condition of the as-rolled sheet to the T8X condition with three levels of forming strain and paint-bake aging. The T8XP condition with enhanced paint-bake response but only one level of forming strain is also considered. The analysis of these panels for deflection under static loading (stiffness) and static denting was undertaken with the implicit finite element code LS-NIKE (Halquist, 1996) while the dynamic denting was modelled with the explicit dynamic finite element code LS-DYNA (Halquist, 1995) followed by a spring back analysis using LS-NIKE3D. The analytical models are those introduced by Jung (2002) and predict denting energy and stiffness by using developed design software.

2. Finite Element Models

Figure 1 shows a schematic of the panel geometry considered. The panels were square with plan dimensions of either 200×200 mm or 600×600 mm. These two sizes are intended to encompass the range of unsupported sheet metal in typical automotive panel assemblies. In addition to flat panels, spherical curvatures of 100, 150, 200, 400, 700, 1000, and 4000 mm radius were considered. The sharper curvatures are representative of sculpted areas within fenders whereas the flatter curvatures are typical of hoods. Panels with double curvatures of unequal radii were also considered.

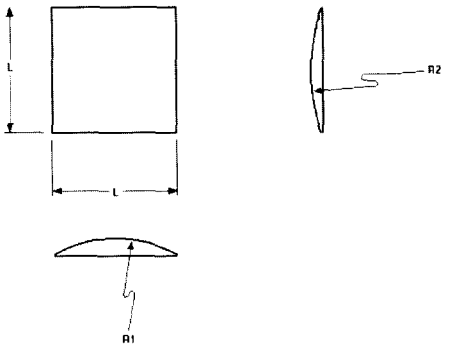

Fig. 1 Schematic of panel geometry adopted in the current study

Figures 2 and 3 show typical finite element meshes used to model the R4000×R4000, 200 mm panel and the R150×R1000, 600 mm panel, respectively. Quarter-symmetry is utilized to reduce the problem size and extensive mesh focussing is employed near the point of load application or impact. Four-node Belytschko-Lin-Tsai (Belytschko et al., 1984; Belytschko and Tsay, 1983) elements were used to discretize the panels. Shell elements were chosen over brick elements due to their greater computational efficiency for modelling thin sheets. Unfortunately, the use of shell elements precludes accurate modelling of through-thickness effects due to transverse compression and shear. Neglecting these terms will result in minor errors in predicted dent depth, primarily for low loads or impact velocities. For higher loads, transverse bending and membrane stretching will control the dent response; these terms are accurately modelled using shell elements. Furthermore, the use of brick elements to capture through-thickness terms would also result in a considerably reduced time step and larger mesh sizes requiring prohibitively long computational times.

A 10×10 grid of 1 mm elements is used at the loading point for all of the models. This consistency in local meshing ensures that the interpolation is constant between models and should eliminate any differences between calculations due to discretization errors. Beyond this regular fine-meshed region, transitional meshes are used for the balance of the sheet geometry. Although

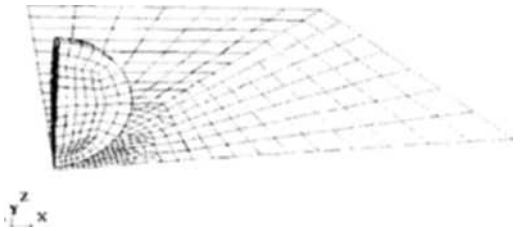

Fig. 2 Finite element mesh used for the R4000× R4000, 200 mm panel

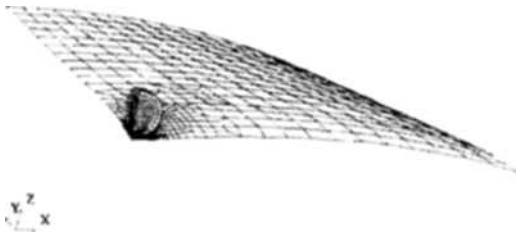

Fig. 3 Finite element mesh used for the R1500× R1000, 600 mm panel

these transitional meshes varied somewhat between calculations, the strain and stress gradients are low away from the load point and so variations in meshing should not be significant.

For the cases in which the radius of curvature was less than one-half of the outer dimension of the 600 mm panel, it was necessary to transition the geometry between a curved region near the impact site and flat region out to the panel boundary. In such cases, a 15 degree arc was used to generate the curved region and the balance of the panel was "extruded" out to the boundary using geometry creation tools available within the pre-processor. Note that the actual curved arc would consist of 30 degrees for the full panel due to symmetry. Figure 3 shows an example of the finite element mesh used for such a geometry, the R150×R1000, 600 mm panel.

Figure 2 also serves to show the mesh used for the impactor in the dynamic denting calculations. The impactor is a 25 mm steel ball bearing. Brick elements were used to discretize the ball and the mesh was focussed somewhat towards the impact face. Note that a rigid body employing only surface discretization near the impact region would likely suffice for these calculations;

however, the calculations were not particularly CPU intensive and a fully discretized indentor would better capture the elastic compliance of the sphere.

2.1 Material properties

The sheet was modelled as elastic-plastic obeying a Mises yield criterion. Anisotropic yield criteria were not adopted since the plastic strains were small. Figure 4 shows the stress-strain data used for these calculations. Effective stress versus plastic strain curves were generated from uniaxial tensile data for the materials modelled. The stress versus plastic strain data was input in a point-wise fashion and linear interpolation was employed between points. The steel sphere was modelled as linear elastic with handbook values assigned for the elastic constants.

As expected, an increase in pre-strain results in a substantial rise in yield stress for the T8X conditions. Tensile data for the T8XP condition was available only for 2% pre-strain material. Comparison of the T8X and T8XP flow stress curves for a similar pre-strain reveals a marked increase in yield stress for the T8XP material. The under-aged T4 condition was merely used as a baseline "soft" material for comparison purposes. Table 1 summarizes the material conditions and yield strengths modelled in the current study.

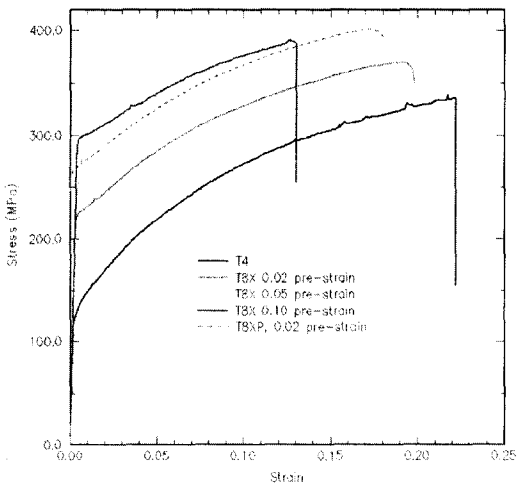

Fig. 4 Stress-strain curves adopted for the sheet materials

Table 1 Yield strength data

Alloy/Temper Designation	Pre-Strain (%)	Yield Strength (MPa)
611-T4	0	127.
611-T8X	2.	222.
611-T8X	5.	252.
611-T8X	10.	295.
611-T8XP	2.	261.

Note that the yield values listed are not 2% offset values, but are the proportional limits (the limits of elasticity) specified in the input data used to describe the uniaxial yield behaviour.

It is interesting to note that the effects of heat treatment and pre-strain appear additive and relatively linear for the AA6111 alloy considered. This observation stems from the similar hardening response of the three pre-strain conditions, after allowing for the initial pre-strain. This behaviour suggests that a relatively simple model could be used to describe the hardening kinetics of deformed panels during the paint-bake cycle.

2.2 Boundary and loading conditions

Standard quarter symmetry conditions were imposed along the symmetry planes. The edges of the panels were modelled as fully clamped ; that is, nodal displacements and rotations were suppressed along the outer edges. Adoption of clamped edge conditions will result in a somewhat stiffer response than using simply supported conditions and hence should be conservative in terms of predicted dent depth, at least for the dynamic denting predictions.

For the static calculations, a load of 155 N was applied to the center of the panel (38.75 N on the quarter-panel modelled). This load was applied incrementally using 10 steps. The load-point deflections at maximum load and at 10% of maximum (after the first increment) were used to calculate panel stiffness (secant). The load was then removed in 10 unloading steps after which the residual deflected shape was used to calculate dent depth as described below.

Note that a nodal point load was used in the

Table 2 Drop height versus impact velocity (neglecting drag.)

Drop Height (mm)	Impact Velocity (m/s)
204	2
1,219	4.89
2,867	7.5
5,097	10

static calculations whereas typical automotive panel performance test standards specify that loading for stiffness measurement is applied through a circular disk and the loading for denting is applied through a sphere. This simplification will result in over-prediction of the actual static deflections and dent depths, but partly counters the effects of the fixed boundary assumption, and was deemed necessary since introduction of the disk-panel and sphere-panel contact conditions would considerably extend and complicate the static analysis.

The dynamic dent calculations considered the impact of a 25 mm steel ball. The impacts were modelled as initial value problems with an initial velocity corresponding to the drop height (Table 2) assigned to the impactor. Penalty function-based contact boundary conditions were defined to enforce intermittent contact between the impactor and panel. The problems were run for a minimum of 5 ms after which the impactor had rebounded off of the panel and the panel was in free vibration. A coupled spring back calculation was then run using LS-NIKE to obtain a final deformed shape after "damping" of the vibrational energy.

2.3 Dent depth

Dent depths were determined from the finite element mesh using a method similar in principle to the dynamic dent measuring procedure used by Thorburn (1994). In that procedure, a dial gauge referenced to three points on the panel, equally around and away from the test point, was used to measure the elevation of the test point before and after impact by the steel ball, the difference being the dent depth, d. In the present analysis, dent depth was calculated by first determining

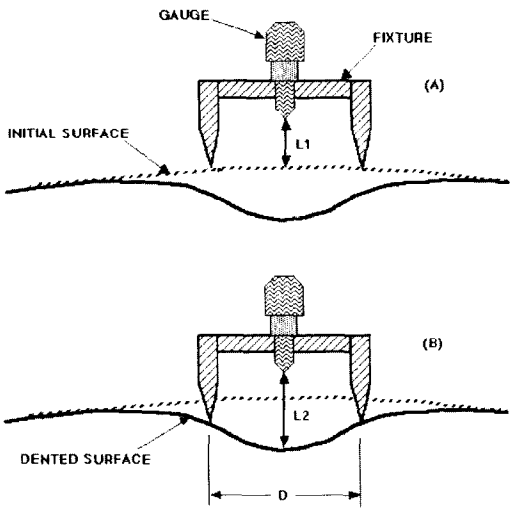

Fig. 5 Schematic of measurements used to calculate dent depth : (a) Bofore and (b) After denting

the difference in height (z-axis) between the node at the center of loading and a point on the panel 12.5 mm away (plan distance along the x-axis) for the original mesh (L1 in Figure 5 (a)), and then comparing it with the corresponding distance calculated for the loaded or impacted mesh (L2 in Figure 5(b)). Linear interpolation between nodes was used to determine panel elevations at the 12.5 mm position. Considering symmetry, this approach would correspond to an actual gauge length, d in Figure 5, of 25 mm.

3. Analysis and Results

The static and dynamic finite element analysis runs were made with the following parametric variations applied to the basic model :

- Panel dimensions of 200×200 or 600×600 mm
- Panel thickness of 0.8, 0.9 or 1.0 mm
- Panel spherical curvatures with radii of 100, 150, 400, 700, 1000, 4000 mm plus a flat panel condition
- Panel double curvatures with unequal combinations of the above radii

- Material yield strength from 127. to 295. MPa due to pre-strain and heat treatment
- Impact velocities of 4.89 m/s plus a range of 2 to 10 m/s

All results are presented graphically. From the static analyses, panel stiffness response is presented in terms of plotted load versus displacement, maximum deflection under load, and secant stiffness. Static denting behaviour is presented using plots of dent depth versus radius of curvature for one strength and all panel sizes and thicknesses. Dynamic denting response is similarly shown using plots of dent depth versus curvature for both sizes and for different strengths. Additional plots show dent depths as a function of impact velocity and double curvature.

3.1 Static response

In Figure 6, the predicted load-deflection curves are plotted for the two sizes of 1 mm AA6111-T8X panels with a full range of spherical radii of curvature. The steeper slopes indicate higher geometric stiffening associated with the smaller radii of curvature, as expected. Comparison of Figures 6(a) and 6(b) reveals that the 600 mm panels are much more compliant than the 200 mm panels. This trend can also be seen in Figure 7 which presents the maximum load-point deflection for all of the calculations.

The load-deflection responses in Figures 6(a) and (b) for the large radius of curvature panels (R=4000 mm) display a number of interesting features not seen in the smaller radii panels. The stiffness or slope is initially high, but drops to a minimum at an inflection point and then increases again. This drop in stiffness is associated with oil canning of the panel as the curvature flattens out and inverts. Once the curvature inverts, then additional load is carried by tensile membrane stresses with an associated increase in stiffness. The high initial stiffness is due to a compressive membrane action prior to oil canning. The stiffness becomes low during oil canning because the panel supports the applied load primarily in bending with a low flexural rigidity. This low bending stiffness is seen in the flat plate

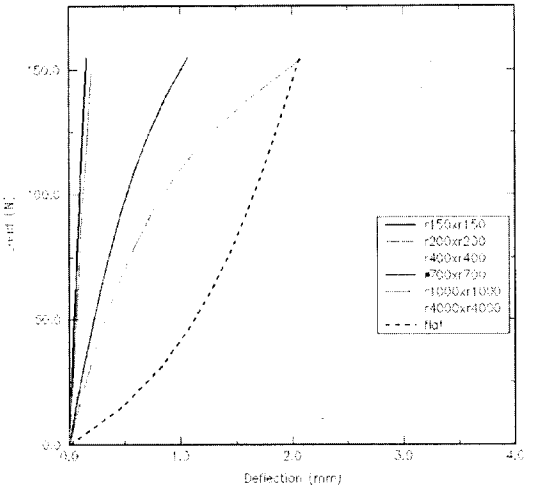

(a) L=200 mm

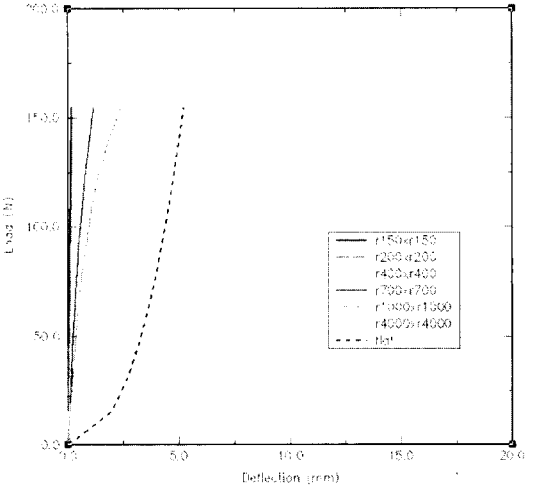

(b) L=600 mm

Fig. 6 Load-displacement response for 6111 T8x, 2% pre-strain, 1 mm panels

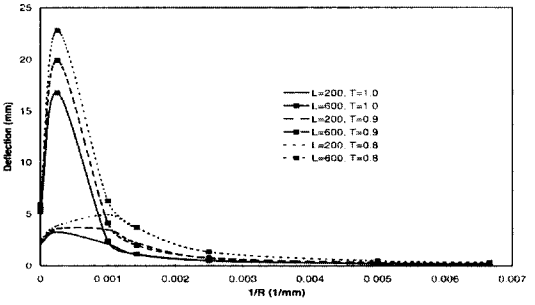

Fig. 7 Maximum load point deflection under a 155 N load. 6111 T8x, 2% pre-strain

predictions where the load carrying is initially only in bending, with no membrane action until there is significant deflection. The panels with a small radius of curvature resist oil canning beyond the 155 N maximum applied load ; thus they remain stiff since loading is supported through membrane compression. Oil canning and subsequent loss of stiffness can be expected to occur at higher loads.

The effect of panel thickness on maximum deflection or compliance is also seen in Figure 7. As expected, the thicker, smaller plates experience lower deflections. The increase in defection for large curvatures is strongly affected by thickness, presumably due to the third order dependence of bending stiffness on thickness. Panel stiffness values are plotted in Figure 8 as the secant stiffness, calculated as the applied load divided by displacement for loads of 155 N and 15.5 N. For the curved panels, the initial stiffness is higher than the stiffness at maximum load due to the geometric softening as the curvature is reduced by the applied load. The flat plates demonstrate a stiffening response, as described above, due to a transition from bending to membrane tension.

3.2 Static dent depth

Predicted dent depths are plotted in Figure 9 for the AA6111-T8X, 2% pre-strain panels subjected to static loading. Dent depth is strongly dependent upon thickness, but not on panel size indicating that it is local bending resistance that controls the depth of static dents for a given material. The sharp curvature panels experience smaller dents since they do not undergo the bending associated with an oil-can mode of deformation. Panels with intermediate curvature exhibited the largest dents since they experience higher bending stresses. In the flatter panels, deflection at lower loads leads to early membrane tension thus minimizing yielding through bending.

3.3 Dynamic dent depths

Figure 10 plots predicted dent depths after

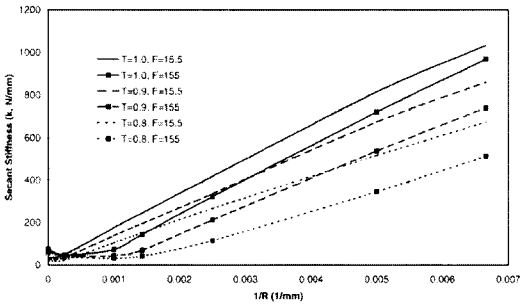

(a) L=200 mm

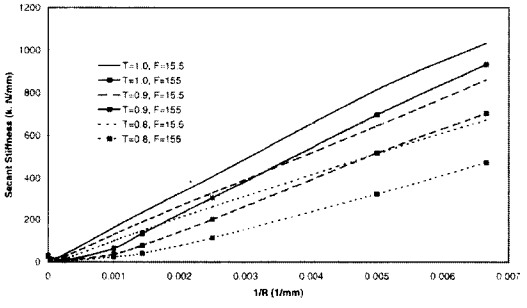

(b) L=600 mm

Fig. 8 Secant siffness (k) as a function of curvature and thickness. 6111 T8x, 2% pre-strain

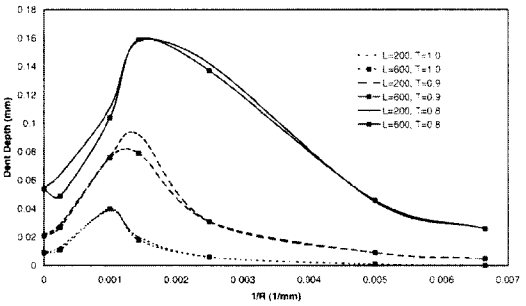

Fig. 9 Static dent depths predicted for the 6111 T8x, 2% pre-strain panels. Maximum load=155 N

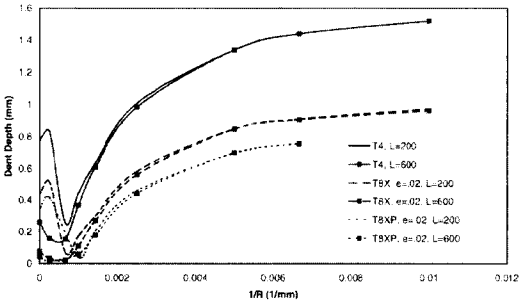

Fig. 10 Dynamic dent depths predicted for the 6111 T8x, 2% pre-strain panels. Impact velocity= 4.89 m/s

dynamic loading by a 4.89 m/s impact of the 25 mm steel sphere on 1 mm spherical curvature panels with different sizes and strengths. The predictions indicate a marked dependence of dent depth on panel strength. There is also a strong non-linear dependency on radius of curvature with a minimum dent depth occurring for the large radii of curvature. Dent depths are large for the sharply curved panels and also for the flat panels. Interestingly, the local minimum dynamic dent depths occur for radii of curvature corresponding to the maximum static dent depths, as seen by comparing Figures 10 and 9. These dramatically different behaviours under static and dynamic loading can be attributed to the influence of panel stiffness on the static and dynamic response. Under static conditions, the stiffer panels tend to resist oil canning thereby limiting bending stresses and minimizing dent depths. For dynamic loading, the more compliant panels are able to elastically absorb more of the impact energy, leaving less energy for the plastic deformation of denting.

The energy absorption ability of a panel subject to a given load will correspond to the area under its load-deflection curve. The static load-deflection curves in Figure 6 indicate that the more sharply curved panels exhibit a stiffer response and absorb less energy for a given load. Consequently, to absorb a given level of impactor kinetic energy, higher contact forces will occur for stiffer panels. The flat panels also show a stiffer response than the R4000×R4000 panels which again leads to higher contact forces and the larger dent depths seen in Figure 10.

Contact force-time histories for an impact velocity of 4.89 m/s are plotted in Figure 11 for the 1 mm AA6111-T8X, 2% pre-strain panels. High contact forces approaching 600 N are attained for the more sharply curved panels. The magnitude of the force decreases and the duration increases as the radii of curvature increase. These general trends are consistent with the load-deformation and stiffness trends seen in Figures 6 and 8, respectively. The flat plates exhibit a lower contact force early in the impact; but later in the impact period, the contact force increases sharply.

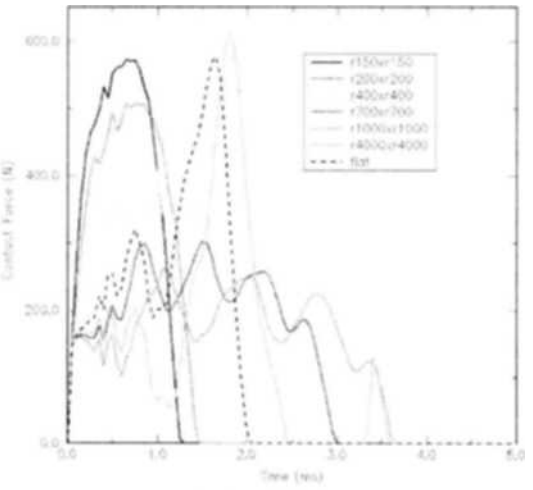

(a) L=200 mm

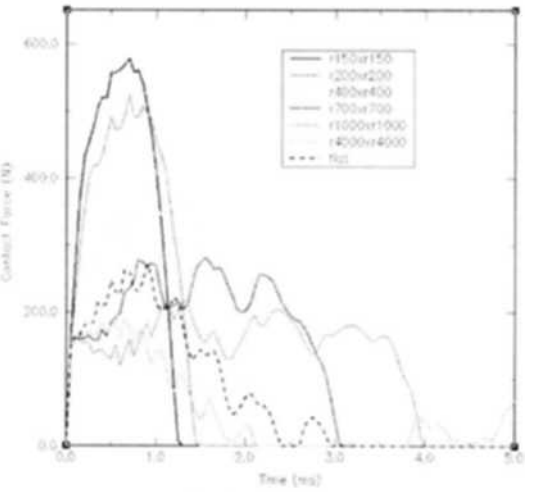

(b) L=600 mm

Fig. 11 Contact force histories for the 1 mm, 6111 T8x, 2% pre-strain panels. Impact velocity= 4.89 m/s

The lower initial forces are attributed to the low initial stiffness of flat panels seen in Figures 6 and 8. The stiffness increases sharply later during the impact as reflected by the hardening of the flat panel load-deformation curves in Figure 6.

3.3.1 Effect of impact velocity

Figure 12 plots predicted dynamic dent depth as a function of impact velocity for flat, AA6111-T8X, 2% pre-strain panels. A velocity range of 2 to 10 m/s was considered, with corresponding

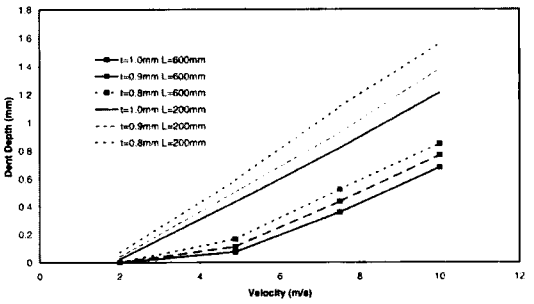

Fig. 12 Dynamic dent depths as function of impact velocity for flat, 6111 T8x, 2% pre-strain panels

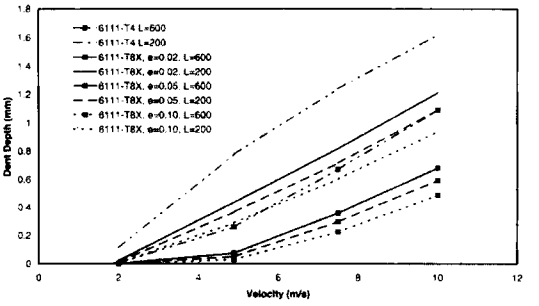

Fig. 13 Dynamic dent depth as a function of impact velocity for 1 mm flat panels comparing various material conditions (heat treatment and pre-strain)

drop heights and kinetic energies summarized in Table 2. For each panel size and thickness, there is an expected increase in dent depth with increased impact velocity. There also exists a threshold velocity (Kohmura and Urbanek, 1977) below which the predicted dynamic dent depth is zero corresponding to the threshold between purely elastic and elastic-plastic impacts.

3.3.2 Panel size effect

Larger dynamic dents are predicted for the smaller 200 mm panel compared to the 600 mm panel. This panel size effect is attributed to the lower stiffness and lower dynamic contact forces for the larger panels. Note that panel size has little influence on static dent depth, seen in Figure 9, since static load level is not coupled to panel stiffness.

3.3.3 Panel thickness and strength effect

Panel thickness has a controlling influence on dynamic dent depth, as is shown for a flat panel in Figure 12, since an increase in section will reduce both bending and membrane stress and thus limit yielding. Increased thickness will contribute to higher stiffness and thus higher contact forces, as will increased curvature, but the effect of thickness on local yielding will dominate. This effect is similar to that seen for static loading in Figure 9.

Predicted dynamic dent depths for 1 mm flat panels with non-heat treated AA6111-T4 and pre-strain AA6111-T8X alloys are plotted in Figure 13. The effect of pre-strain is to increase the yield strength of the panel, as shown by the stress-strain data of Figure 4 and summarized in Table 1, which leads directly to reduced local yielding. The downwards shift of the T8X curves with increased pre-strain is comparable in magnitude to the shift with panel thickness seen in Figure 12. The threshold dent velocity also increases with material strength or pre-strain since the limit for elastic impact increases. The effect of the paint bake treatment on dent resistance is profound as reflected in the dent depths for the T4 condition versus the T8X conditions. Similar effects can be expected for curved panels.

3.3.4 Unequal curvatures

The results presented thus far have considered either flat panels or panels with spherical curvatures (R1=R2). The effect of ellipsoidal or unequal curvatures (R1≠R2) on dynamic dent depth is plotted in Figure 14 for 1 mm, AA6111-T8X panels with 2% pre-strain, impacted at 4.89 m/s. Results for 200 and 600 mm panels are plotted in Figures 14(a) and (b), respectively. In each figure, results are shown for 16 parametric cases using radii of 150, 1000 and 4000 mm, as well as for the flat condition. The diagonal plane (R1=R2) in each plot corresponds to the AA6111-T8X, 1 mm curve in Figure 10. Along the diagonal, the predicted dent depths are shown to be high for stiff sections (R1=R2=150 mm) and a local minimum is seen for R1=R2=4000 mm. The predicted trends off the diagonal (R1≠R2) indicate that the dynamic dent response is

largely controlled by the smallest radius of curvature. For example, the dent depth for the R1=150 mm, R2=4000 mm is very close to the depth for R1=R2=150 mm. In addition, the minimum dent depth for low curvatures appears as a trough in the predicted dent depth "surface". These observations suggest that the R1=R2 results can be used to obtain conservative predictions for unequally curved panels, so long as the minimum radius is used.

Also seen in Figure 14(b) is a large "region" of near-zero dent depth for low curvature or flat panels. In this region, the threshold velocity for plastic deformation is higher than the 4.89 m/s impact considered. The no-denting region is much smaller in Figure 14(a) which presents results from the smaller, stiffer panels which are more easily dented under dynamic loading.

Figure 15 plots dent depths for the same panel geometries as in Figure 14, but considers the weaker T4 condition. As expected, there is a general increase in dent depth due to the lower material strength. For this softer material condition, a region of no-denting does not exist in the plot since the threshold velocity for denting is

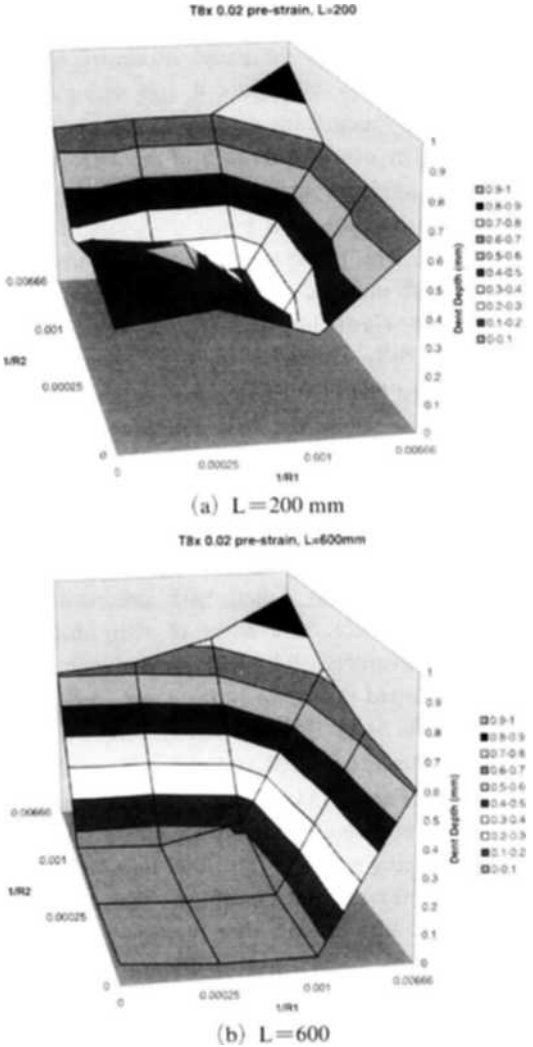

(a) L=200 mm

(b) L=600

Fig. 14 Predicted dynamic dent depths for unequally double curved 6111 T8X, 2% pre-strain panels

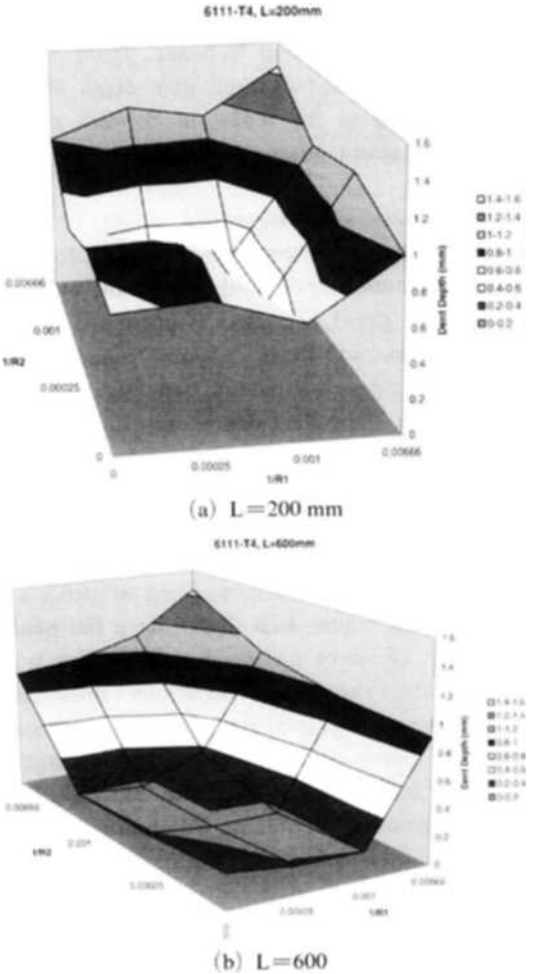

(a) L=200 mm

(b) L=600

Fig. 15 Predicted dynamic dent depths for unequally double curved 6111 T4 panels

exceeded for all of the panel curvatures.

To summarize, the comparisons provided herein do not present a rigorous matching case-by-case assessment of measured versus predicted dent depths and stiffnesses. They do, however, serve to indicate that the ranges of predicted and measured values correspond reasonably well. More importantly, it is shown that the general trends of dent depth dependence on panel stiffness and geometry are consistent.

4. Discussion and Conclusions

The present study has served to demonstrate the complex interdependence of the denting and stiffness response of body panels to material strength, thickness, panel size, curvature, support condition, and loading. Of particular interest is the competitive nature of dynamic versus static-dent performance. Panels of high local curvature and stiffness will perform well under static loading, but will be susceptible to poor dynamic dent performance due to an inability to elastically absorb the kinetic energy of an impacting body. Designers must be aware of this competition in optimization and trade-off studies involved in panel design.

The results presented in this study should also be of use in studies of down-gauging potential of existing designs. Unfortunately, given the number of variables involved in body panel design, the current study is limited and consideration should be given to incorporating the effects of other parameters such as support conditions, panel sizes, and impact locations that are off-center, for example. For comparison or material ranking purposes, calculations utilizing steel properties should also be undertaken. From above study, the following conclusions can be summarized as like ;

(1) Panel stiffness and dent performance exhibit a complex dependence upon panel size, curvature, and thickness ; denting has a further strong dependence on loading and material strength.

(2) Static and dynamic dent resistance improve with increased panel thickness and material yield strength.

(3) Panel stiffness and static dent performance are enhanced by curvatures which favor membrane loading as opposed to bending.

(4) Stiff panels, that is, sharply curved and smaller panels, experience higher contact forces for a given impact and dent more easily. Thus static and dynamic dent performance must be treated as conflicting requirements during panel design.

Acknowledgment

This work was supported by a grant from the Chuongbong Academic Research Fund of the Cheju National University Development Foundation.

References

Belytschko, T., Lin, J. I. and Tsay, C., 1984, "Explicit Algorithms for the Non-Linear Dynamics of Shells," *Computer Methods in Applied Mechanics and Engineering*, Vol. 42, pp. 225~251.

Belytschko, T. and Tsay, C., 1983, "A Stabilization Procedure for the Quadrilateral Plate Element with One-Point Quadrature," *International Journal for Numerical Methods in Engineering*, Vol. 19, pp. 405~419.

Burley, C. E., Niemeier, B. A. and Koch, G. P., 1976, "Dynamic Denting of Autobody Panels," *SAE Technical Paper* No. 760165.

Burley, C. E. and Niemeier, B. A., 1977, "Denting Properties of Aluminum Autobody Components," *SAE Technical Paper* No. 770199.

DiCello, J. A. and George, R. A., 1974, "Design Criteria for the Dent Resistance of Auto Body Panels," *SAE Technical Paper* No. 740081.

Ekstrand, G. and Asnafi, N., 1998, "On Testing of the Stiffness and the Dent Resistance of Autobody Panels," *Materials and Design 19*.

Halquist, J. O., 1996, "LS-NIKE3D User's Manual," *LSTC Report 1016, Livermore Software Technology Corporation*, Livermore, CA.

Halquist, J. O., 1995, "LS-DYNA3D User's

Manual," *LSTC Report 1082, Livermore Software Technology Corporation*, Livermore, CA.

Johnson, T. E. and Schaffnit, W. O., 1973, "Dent Resistance of Cold-Rolled Low-Carbon Steel Sheet," *SAE Technical Paper* No. 730528.

Jung, D. W., 2002, "A Parametric Study of Sheet Metal Denting Using a Simplified Design Approach," *KSME International Journal*, Vol. 16, No. 12, pp. 1479~1492.

Kohmura, S. and Urbanek, J., 1977, "Dent Resistance of Aluminum Alloy Sheets," Alcan International Ltd., KRDC Report, KR-77/044.

Mahmood, H. F., 1981, "Dent Resistance of Surface Panel and Slam Area," *SAE Technical Paper* No. 810099.

Neimeier, B. A. and Burley, C. E., 1978, "Hailstone Response of Body Panels — Real and Simulated," *SAE Technical Paper* No. 780398.

Rolf, R. L., Sharp, M. L. and Stroebel, H. H., 1976, "Structural Characteristics of Aluminum Body Sheet," *SAE Technical Paper* No. 770200.

Shi, M. F., Brindza, J. A., Michel, P. F., Bucklin, P., Belanger, P. J. and Prencipe, J. M., 1997, "Static and Dynamic Dent Resistance Performance of Automotive Steel Body Panels," *SAE Technical Paper* No. 970158.

Swenson, W. E. and Traficante, R. J., 1982, "The Influence of Aluminum Properties on the Design, Manufacturability and Economics of an Automotive Body Panel," *SAE Technical Paper* No. 820385.

Thomas, D., Hodgins, R. B., Worswick, M. J., Oddy, A. S., Gong, K. and Finn, M., 1999, "FEM Technique for Static & Dynamic Dent Modelling of Aluminum," *Proceedings of Numisheet '99 — Volume 1*, Gelin, J. C. and Picart, P., Eds., pp. 367~372.

Thorburn, H. J., 1994, "Comparitive Tests of Stiffness and Dent Resistance on Aluminum and Steel Fenders," *Proceedings IBEC '94, International Body Engineering Conference*, pp. 105~112.

Vadhavkar, A. V., Fecek, M. G., Shah, V. C. and Swenson, W. E., 1981, "Panel Optimization Program (POP)," *SAE Technical Paper* No. 810230.

Vreede, P. T., Tamis, P. J. and Roelofsen, M. E., 1995, "The Influence of Material Properties and Geometry on Dynamic Dent Resistance : Experiments and Simulations," *Proceedings IBEC '95, International Body Engineering Conference*, pp. 79~86.